Reactions of DOPA (3,4-Dihydroxyphenylalanine) Decarboxylase with DOPA

By Alba MINELLI,* Alan T. CHARTERIS,* C. BORRI VOLTATTORNI† and Robert A. JOHN*
*Department of Biochemistry, University College, P.O. Box 78, Cardiff, CF1 1XL, Wales, U.K., and
†Institute of Biological Chemistry, University of Perugia, Perugia, Italy*

The study of DOPA (3,4-dihydroxyphenylalanine) decarboxylase by steady-state methods is difficult because multiple reactions occur. The reaction with DOPA was studied at enzyme concentrations between 20 and 50 μM by direct observation of the bound coenzyme by using stopped-flow and conventional spectrophotometry. Four processes were observed on different time scales and three of these were attributed to stages in the decarboxylation. The fourth was attributed to an accompanying transamination that renders the enzyme inactive. It was clear that much, if not all, of the 330 nm-absorbing coenzyme present in the free enzyme plays an active part in the decarboxylation, since it is converted into 420 nm-absorbing material in the first observable step. An intermediate absorbing maximally at 390 nm is formed in a slower step. Rate and equilibrium constants have been determined and the ratio of decarboxylation to transamination was estimated to be 1200:1.

Several reports have described homogeneous preparations of DOPA (3,4-dihydroxyphenylalanine) decarboxylase (EC 4.1.1.28) from pig kidney. From these reports it is clear that the enzyme contains tightly bound pyridoxal phosphate as cofactor (Christenson *et al.*, 1972; Borri Voltattorni *et al.*, 1971, 1979; Lancaster & Sourkes, 1972). The enzyme is difficult to study by using steady-state kinetics because as well as catalysing the decarboxylation of DOPA, it also catalyses a decarboxylation-dependent transamination. This reaction, because it converts the bound coenzyme into pyridoxamine phosphate, inactivates the enzyme with a half-time of a few minutes (O'Leary & Baughn, 1975, 1977). Pyridoxal phosphate can be used to reactivate the enzyme, but this introduces further complications that result from the combination of DOPA with the unbound coenzyme in a Pictet–Spengler reaction, a reaction that entails ring closure to give an isoquinoline and that is attributable to the directive effects of the *m*-hydroxy group in the catechol ring (Pictet & Spengler, 1911; Whaley & Govindachari, 1951; Schott & Clark, 1952; O'Leary & Baughn, 1977).

The present paper reports investigations into the mechanism of DOPA decarboxylase by using the absorption spectrum of the bound coenzyme as an indicator of events. By using suitable reactant concentrations and both conventional and stopped-flow spectrophotometry, we have been able to study the decarboxylation and transamination reactions separately.

Experimental

Materials

DOPA decarboxylase was prepared by one of two methods. For most of the experiments reported in the present paper we used a preparation made in the Institute of Biological Chemistry, University of Perugia, Perugia, Italy, by the method of Borri Voltattorni *et al.* (1979). This method gives a relatively high yield (130 mg from eight kidneys) of enzyme that, on sodium dodecyl sulphate/polyacrylamide-gel electrophoresis, shows two bands of roughly equal intensity. For some exploratory stopped-flow experiments, and for those experiments described in the section on transamination, we used an enzyme preparation obtained by a modification of the method of Borri Voltattorni *et al.* (1979) described previously (John *et al.*, 1978). This preparation gave a much lower yield (10 mg from six kidneys) of enzyme that is homogeneous on sodium dodecyl sulphate/polyacrylamide-gel electrophoresis and appears to be composed of two monomers with the same molecular weight of 56000. This is the approximate molecular weight of the larger of the two bands present in the other preparation. Both preparations, however, were kinetically identical.

DOPA was from Koch–Light Laboratories, Colnbrook, Bucks., U.K. The purity of this material was checked by t.l.c. with fluorescent silica gel (HF$_{254+366}$, type 60; E. Merck, Darmstadt, Germany) and butanol/acetic acid/water (3:1:1, by vol.) as

solvent. Only one u.v.-absorbing component was present and comparisons of the A_{280} for solutions of this compound with that expected from the absorption coefficient ($\varepsilon_{280} = 2630$ litre·mol^{-1}·cm^{-1}; Stecher, 1968) showed it was better than 98% pure.

Other chemicals were bought from BDH Chemicals, Poole, U.K.

Spectrophotometry

Stopped-flow experiments were carried out by using a Durrum Gibson stopped-flow spectrophotometer and the results were recorded by photographing the display of a Tektronix R.M. 564 storage oscilloscope.

Slower reactions and absorption spectra were determined in a Beckman model 25 recording spectrophotometer.

Measurement of apparent first-order constants

Reactions that appeared first order were analysed in two ways.

Method 1. When the end point of a reaction was clear, the first-order nature of the reaction was checked by a logarithmic plot. The best value for $k_{obs.}$, the observed rate constant, was then determined by a linear least-square regression analysis. Where error bars are shown in the relevant figures they indicate standard deviations obtained from several such determinations of $k_{obs.}$. Where error bars are not shown, each point indicates a single such determination.

Method 2. When the end of the reaction was not directly determinable because of the onset of another reaction, $k_{obs.}$ was determined by using the estimated end point that gave the highest correlation coefficient after linear regression analysis.

Fitting integrated equations

The concentration of ES complex, x, in that part of the reaction referred to as the final phase was predicted by using eqn. 1:

$$x = \frac{es}{K_m(1+p/K_p)+s} \qquad (1)$$

The concentrations of substrate, product and active enzyme at any time are represented by s, p and e. K_m and K_p are apparent dissociation constants for substrate and product. Values of e, s and p were determined by numerical integration of eqns. (2) and (3) by using a programmable calculator and a process of reiteration.

$$-\delta e = k_1 \delta t \qquad (2)$$

$$-\delta s = \delta p = k_{cat.} \, x \, \delta t \qquad (3)$$

The time interval, δt, used for each iteration was 1 ms. This value is 300-fold smaller than the reciprocal of the fastest rate constant.

Determination of enzyme concentration

Enzyme concentrations are expressed as bound coenzyme determined by releasing the bound pyridoxal phosphate into strong base by treating 0.4 ml of enzyme in 0.05 M-sodium phosphate buffer with 10 μl of 10 M-NaOH. Pyridoxal phosphate concentration was measured by using $\varepsilon_{388} = 6600$ litre·mol^{-1}·cm^{-1} (Peterson & Sober, 1954).

Results

The absorption spectrum of the free enzyme shows peaks at 333 nm and at 420 nm (Borri Voltattorni, et al., 1971). When the pH is increased in the range 6.5–8.5 the 333 nm peak increases at the expense of the peak at 420 nm (Fiori et al., 1975; Borri Voltattorni et al., 1979).

When the enzyme is made alkaline (pH > 12) the coenzyme is released and shows the characteristic absorbance of free pyridoxal phosphate with a peak at 388 nm (Fig. 1a). The complete disappearance of both the 333 nm and 420 nm peaks indicates that all the coenzyme is released by this treatment.
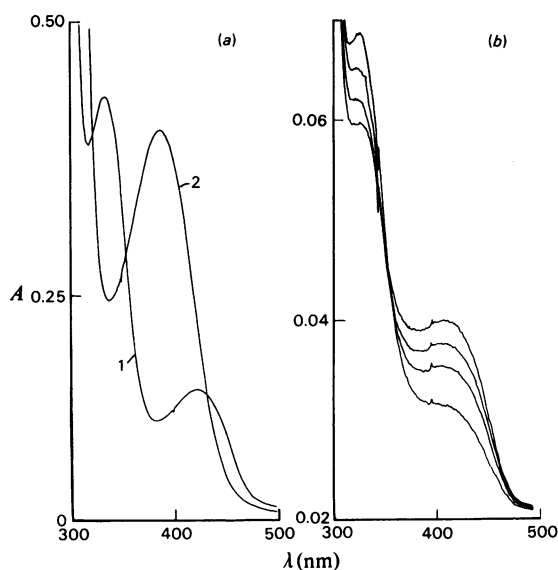

Fig. 1. *Absorption spectra of DOPA decarboxylase* (a) Spectrum of enzyme in 0.05 M-sodium phosphate, pH 7, before (1) and after (2) treatment with 10 μl of 10 M-NaOH. (b) Spectral changes associated with transamination. The enzyme (9 μM) was treated with 16.6 mM-DOPA and absorption spectra were recorded 2, 5, 12 and 20 min after the start of the reaction (scan time = 2 min). The spectrum with highest absorbance at 420 nm is that at the start of the reaction and the remaining spectra are in order of decreasing absorbance at this wavelength. The spectra were recorded in 85 mM-sodium phosphate buffer, pH 7.0, 25°C.

Transamination

O'Leary & Baughn (1977) showed that decarboxy-lation-dependent transamination accompanies simple decarboxylation by demonstrating that dihydroxy-phenylacetaldehyde was produced during the action of the enzyme on DOPA. These workers also esti-mated the rate of the transamination by measuring the amount of pyridoxal phosphate needed to restore activity to enzyme that had become inactive by transamination. We have confirmed and extended the results of O'Leary & Baughn (1977) by following changes in the spectrum of the bound coenzyme as it transaminates. By using high concentrations of DOPA the enzyme can be maintained close to saturation for many minutes and changes in the absorption spectrum due to transamination can be followed (Fig. 1b). We have also followed the course of this reaction contin-uously at 420nm by using [DOPA] = 28 mM. This concentration is sufficient to maintain more than 95% saturation of the enzyme throughout and the rate constant was found to be $2.2 \times 10^{-3} s^{-1}$ at 25°C and $5.4 \times 10^{-3} s^{-1}$ at 37°C.

Most of the experiments described in the present paper were of such short duration that the trans-amination was negligible.

Summary of spectral changes seen after rapid mixing

When the enzyme is mixed with DOPA in the stopped-flow apparatus, and the reaction course determined at 420nm, three events can be seen (Fig. 2). A fast ($t_{\frac{1}{2}} < 5$ ms) apparently first-order reaction in which A_{420} increases (a), is followed by a slower process ($t_{\frac{1}{2}} \sim 20$ ms) in which A_{420} decreases (b). The final process (c) also gives decreasing A_{420} and the course of the reaction resembles that expected for the decay of the ES complex as substrate concentration decreases from well above the value for K_m to zero. At 330nm the direction of the fast and final processes are reversed.

Under appropriate conditions these reactions occur at sufficiently different rates to permit their separate examination.
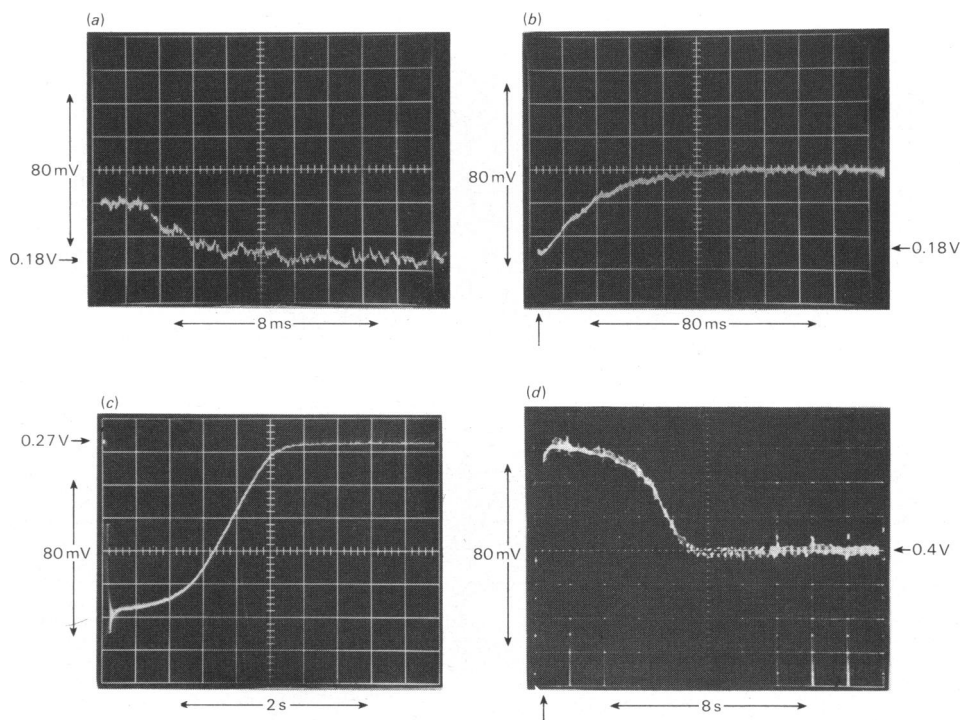

Fig. 2. *Transmission changes at 420 and 330nm*

Three events are detected at 420nm when DOPA decarboxylase is mixed with DOPA in the stopped-flow apparatus at 24°C. The direction of the fastest and slowest changes is reversed at 330nm. (a) 420nm, 50 μM-enzyme, 0.1 mM-DOPA; (b) 420nm, 27 μM-enzyme, 1 mM-DOPA; (c) 420nm, 54 μM-enzyme, 1 mM-DOPA; (d) 330nm, 27 μM-enzyme, 1 mM-DOPA. All reactions were carried out in 0.05 M-sodium phosphate buffer, pH 7.
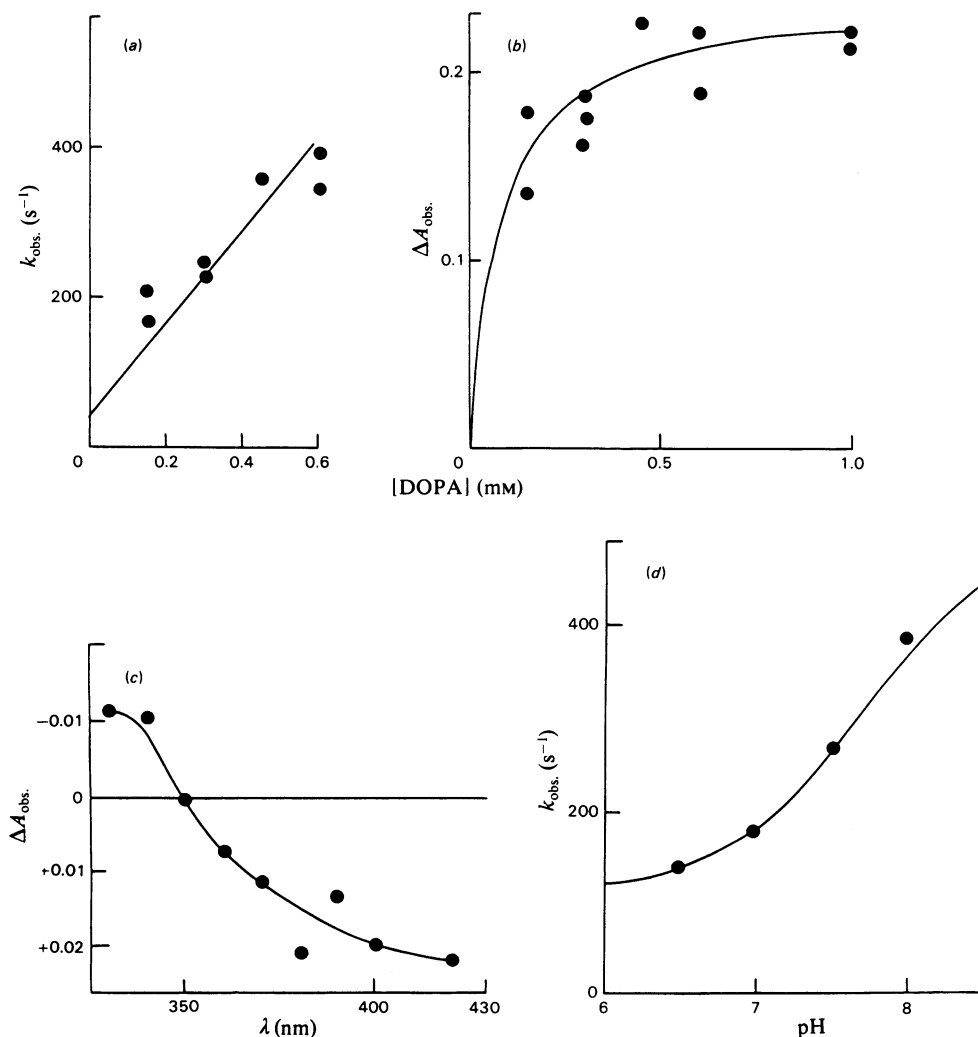
Fig. 3. *Properties of the fast reaction*

(a) Variation of $k_{obs.}$ with substrate concentration. Conditions were: enzyme, $55\,\mu M$; pH7; 420nm. Values of $k_{obs.}$ were determined as described in method 1 under 'Measurement of apparent first-order constants'. (b) Variation of amplitude of absorbance changes, $\Delta A_{obs.}$, with substrate concentration. Conditions were as in (a). (c) Difference spectrum. The change in total absorbance was measured at different wavelengths. Conditions were: DOPA, 0.1mM; enzyme, $13\mu M$; pH7.0. (d) Variation of $k_{obs.}$ with pH. Conditions were: DOPA, 0.1mM; enzyme, $40\mu M$, 420nm. The solid line is theoretical from $k_{obs.} = k_E/[(K/[H^+])+1]+k_{EH+}/[([H^+]/K)+1]$ with $k_E = 600s^{-1}$, $k_{EH+} = 140s^{-1}$ and p$K = 7.7$. All reactions were carried out in 0.05 M-sodium phosphate.

The fast reaction

At substrate concentrations above 0.6mM this reaction becomes too fast to follow in our stopped-flow apparatus and below 0.1mM it becomes sig-significantly affected by the next process. We have determined the dependence of the apparently first-order rate constant ($k_{obs.}$) and amplitude ($\Delta A_{obs.}$) for this reaction on substrate concentration (s_0) and the results are shown in Fig. 3. The lines drawn through the points were derived assuming that $k_{obs.} = k_{+1}s_0 + k_{-1}$ and that $\Delta A_{obs.} = \Delta A_0 k_{+1}s_0/(k_{-1}+k_{+1}s_0)$ by using the values $k_{+1} = 6\times 10^5 M^{-1}s^{-1}$, $k_{-1} = 50$ s^{-1} and $\Delta A_0 = 0.24$. When $s_0 \gg e_0$ these relationships are consistent with eqn. (4):

$$E+S \underset{k_{-1}}{\overset{k_{+1}}{\rightleftharpoons}} ES \qquad (4)$$

It is noteworthy, however, that, at the lowest substrate concentrations used, s_0 was only about $4e_0$ and that other interpretations are also consistent with the rather scattered experimental points in Fig. 3.

The difference spectrum shown in Fig. 3(c) was obtained by measuring the amplitude of the fast reaction at different wavelengths. At 350 nm there was no detectable absorbance change and below 350 nm the direction of the absorbance change was clearly reversed.

Fig. 4. *Properties of the slower reaction*
(a) Variation of $k_{obs.}$ with substrate concentration. Conditions were: enzyme, $55 \mu M$; pH 7.0; 420 nm. Values of $k_{obs.}$ are means for three determinations as described in method 1 under 'Measurement of apparent first-order constants', except that for [S] = 0.45 mM $k_{obs.}$ is the result of a single determination and for [S] = 0.15 mM method 2 was used. (b) Difference spectrum. Each point represents a single determination of the total absorbance changes, $\Delta A_{obs.}$, at each wavelength. The continuous line was constructed by assuming conversion of a compound with $\lambda_{max.}$ 420 nm into a compound with $\lambda_{max.}$ 390 nm, having the same extinction coefficient. The actual, rather than the net, absorbance change was assumed to be 0.045 at $\lambda_{max.}$ in each case. All determinations were in 0.05 M-sodium phosphate at 24°C.

The pH dependence of this reaction was studied in the pH range 6.5–8.0 by using a substrate concentration of 0.1 mM and measuring at 420 nm. The results are shown in Fig. 3(d). We could not carry out experiments outside this pH range because below pH 6.5 the enzyme is unstable and above pH 8.0 the reaction is too fast. From the limited data it appears that two ionic forms of the enzyme react with the substrate and that the unprotonated form reacts above five times more rapidly than the protonated form.

The slower reaction

This reaction was clearly separable in time scale from the faster reaction preceding it at all the enzyme and substrate concentrations studied. However, it merges into the final phase when enzyme concentration is increased and when substrate concentration is decreased. The conditions used to give the results of Fig. 4 were chosen with this consideration in mind. The reaction-difference spectrum (Fig. 4b) is best interpreted by proposing that a compound absorbing maximally at 420 nm is converted into a compound absorbing maximally at 390 nm.

The dependence of $k_{obs.}$ on substrate concentration (Fig. 4b) suggests simple saturation kinetics, except that at high substrate concentration there may be some inhibition. However, if the decrease in $k_{obs.}$ seen between 1 mM and 5 mM is attributed to experimental error and the data are analysed by the method of Wilkinson (1961) the dissociation and rate constants are respectively $K_d = 0.5 \pm 0.1$ mM (mean $\pm$ s.D.) and $k = 53 \pm 3$ s^{-1} (mean $\pm$ s.D.).

We have measured both the total absorbance change, ΔA_0, and $k_{obs.}$ at different pH values by using 1 mM-DOPA and $27 \mu M$-enzyme. At pH 7, 7.5 and 8.0 these values are the same [$\Delta A_0 = 0.07$; $k_{obs.} = 35 \pm 5$ s^{-1} (mean $\pm$ s.D.)]. However, at pH 6.5 ΔA_0 is significantly decreased to 0.04 and the reaction is faster [$k_{obs.} = 61 \pm 13$ s^{-1} (mean $\pm$ s.D.)]. The decreased extent and increased rate of the reaction seen at low pH are most readily explained by assuming that the step is reversible and that the rate of the back reaction becomes significant below pH 7.

The final phase

The last 20% of the amplitude of this phase follows first-order kinetics and $k_{obs.}$ is proportional to enzyme concentration, e_0. However, for any given enzyme concentration, when the initial substrate concentration, s_0, was below 0.5 mM the observed rate constant was independent of substrate concentration. It seems probable that this phase is due to the simultaneous decrease in the concentration of the various ES complexes as the substrate concentration, s, decreases
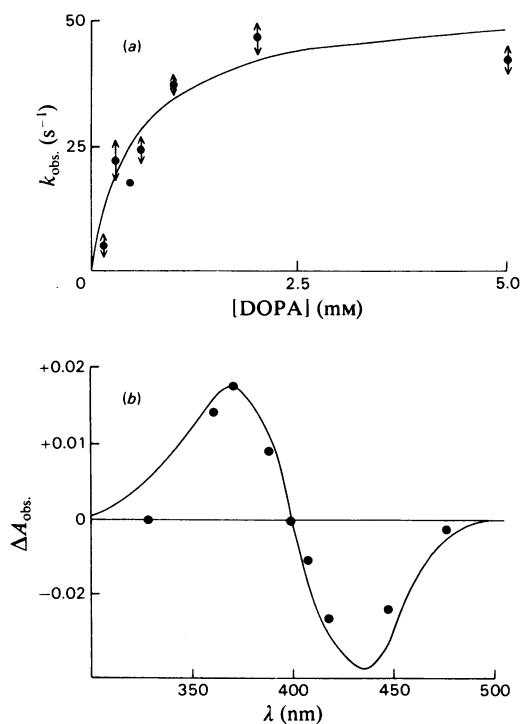
from well above K_m to zero. In this case the first-order rate constant observed at the end is given by $k_{obs.} = k_{cat.} \cdot e_0/K_m$. Measurements of $k_{obs.}$ for several different enzyme concentrations between $20\,\mu M$ and $50\,\mu M$ gave a value of $k_{cat.}/K_m = 6.8 \pm 0.6 \times 10^4 M^{-1} \cdot s^{-1}$ (mean $\pm$ S.D.).

Fig. 5 shows the absorbance changes seen at 420 nm when the enzyme was mixed with 1 mM- and 5 mM-DOPA. At these concentrations the reaction lasts long enough for transamination to result in significant inactivation. In addition the product concentrations are relatively high. We have therefore used an integrated equation that incorporates both progressive loss of enzyme activity and product inhibition to fit the data (see the Experimental section).

The continuous lines of Fig. 5 were derived by using $k_{cat.} \cdot e_0 = 88\,\mu M \cdot s^{-1}$, $K_m = 80\,\mu M$ and the inactivation rate constant, k_i, $= 2.2 \times 10^{-3} s^{-1}$, determined independently as described above. The value used for the inhibition dissociation constant was $K_p = 10 mM$. The enzyme concentration, determined on the same enzyme sample by release of coenzyme with NaOH, was $27\,\mu M$ and thus $k_{cat.} = 3.3 s^{-1}$. The value obtained for $k_{cat.}/K_m$ on this basis ($4.1 \times 10^4 M^{-1} \cdot s^{-1}$) is a little lower than that obtained in separate experiments analysing only the last part of the reaction as described above.

The difference spectrum for this phase was almost exactly the reverse of that obtained for the fast reaction.
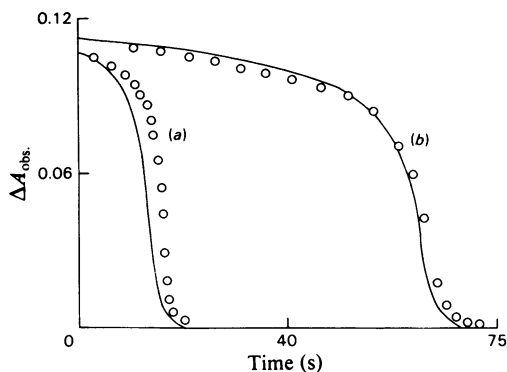

Fig. 5. *The final phase*
The complete reaction observed at 420 nm using (*a*) 1 mM-DOPA and (*b*) 5 mM-DOPA. Conditions were: enzyme, $27\,\mu M$; pH 7.0; sodium phosphate buffer, 0.05 M; 24°C. The points are experimentally determined values of absorbance change taken from oscilloscope traces showing transmission. The continuous line is determined from eqns. (2) and (3) as described in the Experimental section by using the values given in the Results section.

Discussion

The presence of two absorbance bands above 300 nm in the free enzyme shows that the coenzyme must be present in at least two forms (Heinert & Martell, 1963). The coenzyme is bound as an internal aldimine with a lysine residue of the enzyme protein (Bossa *et al.*, 1977) and by analogy with model compounds the 420 nm absorbance can be attributed to the protonated aldimine indicated as the mesomeric structure (I) of Fig. 6 (Heinert & Martell, 1963).

Assignment of the 333 nm band is less easy because so many forms of the coenzyme absorb maximally in this region (Johnson & Metzler, 1970). Borri Voltattorni *et al.* (1979) have shown that the 420 nm peak decreases and the 333 nm peak increases as the pH is raised in the range 6.5–8.5. It is clear from the results reported in the present paper that the coenzyme absorbing at 333 nm is reactive because it is decreased in the fast reaction and reappears in the final phase. Furthermore, since we see a 5-fold increase in the rate of the fast reaction as the pH is raised from 6.5 to 8.0, we infer that it is the 333 nm-absorbing form that forms the initial aldimine with the substrate.

Glutamate decarboxylase shows very similar pH-dependent spectral changes (Shukuya & Schwert, 1960) and O'Leary (1971) has suggested that the 330 nm absorbance of this enzyme is due to an aldamine (III) in which the second nitrogen atom on C-5' comes from a second enzyme lysine residue. The pH-dependence of the spectrum is attributed by O'Leary (1971) to protonation of this second lysine residue which prevents aldamine formation and leaves 420 nm-absorbing aldimine. The reactivity of the 333 nm-absorbing form rules out this possibility for DOPA decarboxylase.

It is well established that the 330 nm-absorbing tautomer (II) of the protonated aldimine (I) predominates in a non-polar environment (Heinert & Martell, 1963; Johnson & Metzler, 1970; Feldman & Helmreich, 1976; Gani *et al.*, 1978). One proposal consistent with all the results is therefore that the 333 nm absorbance is due to coenzyme buried in a hydrophobic pocket, the existence of which depends, via a conformational change, on an ionization occurring in the pH region 6.5 to 8.5.

If it were not for the low wavelength of maximal absorbance, the simplest explanation for the 333 nm chromophore would be that it is due to the unprotonated aldimine. The pH-dependent changes in spectrum and rate constant would then be due simply to the protonation of the aldimine.

Although most model unprotonated aldimines have absorbance maxima in the region of 360 nm there is considerable variation. Decreased coplanarity of the resonant system has been suggested by Johnson & Metzler (1970) as an explanation for the low $\lambda_{max.}$ of pyridoxylidene leucine (343 nm)
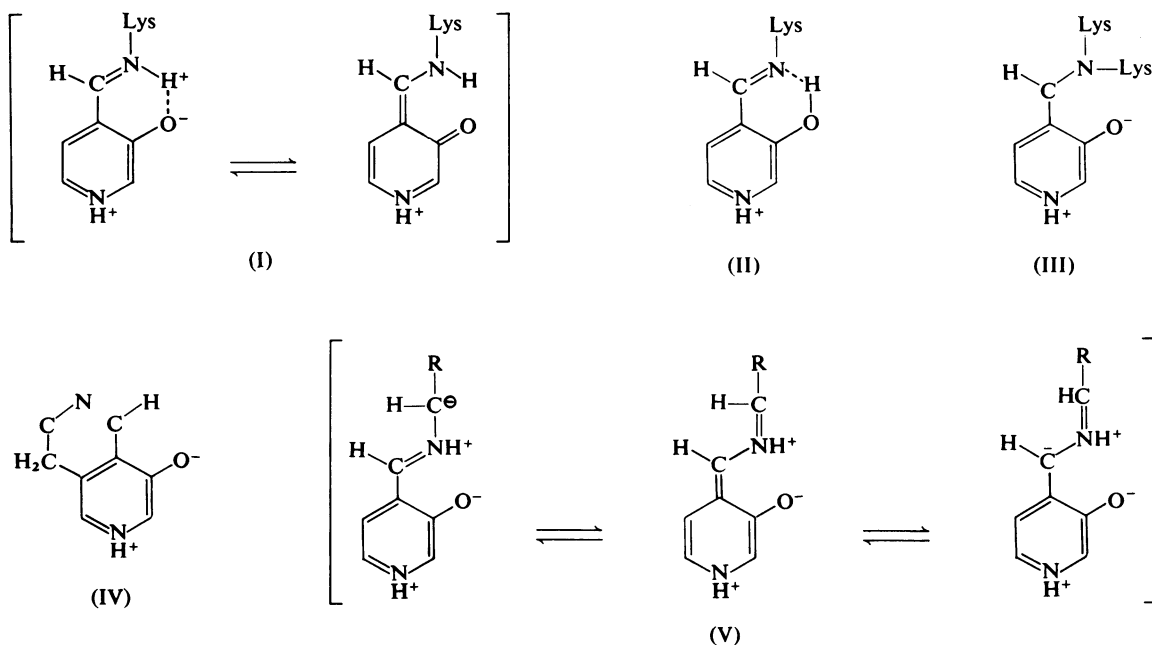
Fig. 6. *Structures of some relevant pyridoxal derivatives*

The 2-methyl and 5-phosphohydroxymethyl substituents have been omitted for simplicity except in structure (IV), where only the 2-methyl group has been omitted.

compared with that of pyridoxylidene valine (367 nm) and this seems to be supported by the observation that when rotation is prevented, as in 7,8-dihydro-3-methyl-2,6-naphthyridin-4-ol, the unprotonated imine (IV) has a still higher absorbance maximum (375 nm; Fisher & Metzler, 1969). Since the contribution of the very large aromatic amino acid absorbance due to the DOPA decarboxylase protein is greater on the low-wavelength side of the 333 nm-absorbance peak, the true $\lambda_{max.}$ due to coenzyme alone must be nearer 340 nm. We therefore suggest that the form of the coenzyme that reacts with the substrate is the unprotonated aldimine the resonance system of which is distorted from planarity by interaction with the protein.

It seems probable therefore that the initial fast reaction is the formation of an 'external' aldimine with the substrate and that at the pH of our experiments this aldimine is almost fully protonated, thus absorbing more at 420 nm than the internal aldimine. If our interpretation of the data of Fig. 2 is correct then the unprotonated aldimine is about 5-fold more reactive than the protonated form. These reactions and associated ionizations are shown as steps (1)–(4) of eqn. 5.

The evidence for the inclusion of step (5) of eqn. 5 is not strong. If the compound formed in the initial fast reaction is the same as that which undergoes the slower reaction, then A_0 for the fast step would show the same substrate concentration dependence as $k_{obs.}$
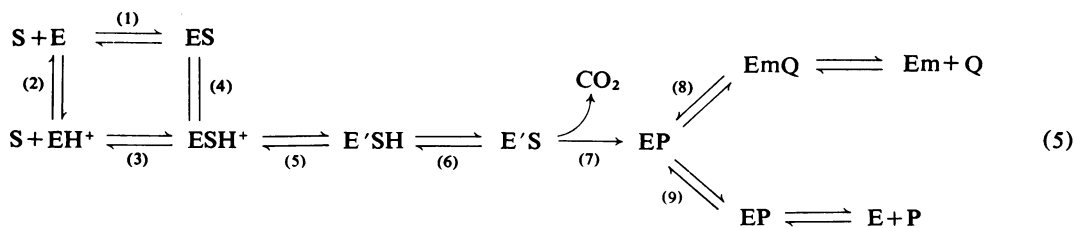
for the slower step. Because the 6-fold difference between the apparent dissociation constants for these two steps seems outside the range of the errors we have included step (5) and suggest an equilibrium constant of about 0.13 for it. However, we can make no suggestion for the nature of the reaction itself.

The apparent reversibility of the slower reaction suggests that it precedes the bond-breaking step (it seems improbable that loss of the carboxy group would be significantly reversible). In addition the difference spectrum for the reaction shows that a compound with an absorbance maximum in the range 380–390 nm is formed whereas the quinonoid-anionic structure (IV), which would be formed immediately after decarboxylation, would absorb at about 490 nm (Schirch & Jenkins, 1964; Fasella, 1967; Braunstein, 1973). If this step precedes decarboxylation the 390 nm-absorbing material produced must be another form of the external aldimine. Complexes absorbing maximally at 385 nm have been observed for poorer substrates with DOPA decarboxylase by Fiori et al. (1975), and Matsushima & Martell (1967 a,b) have observed a very similar absorption band for the metal chelates of unprotonated model pyridoxaldimines. This chelation increases the lability of the substituents on the α-carbon atom of the amino acid and it may be that the 420 nm-to-390 nm transition produces an analogous reactive intermediate (step 6).

There remains the assignment of the rate-limiting step of about $3 s^{-1}$. It seems likely that this is the decarboxylation step itself (step 7) and that it is not directly visible because the quinonoid-carbanion intermediate formed (V) does not accumulate, presumably because of rapid protonation in the next step. However, the fate of this intermediate decides whether simple decarboxylation or decarboxylation-dependent transamination occurs. Protonation at the α-carbon atom of the substrate leads to regeneration of the active aldimine enzyme (step 8), whereas protonation of c-5' of the coenzyme leads to the inactive pyridoxamine form (step 9). Although we cannot measure the absolute values of the rate constants, we estimate that the α-carbon atom of the substrate is favoured in the ratio 1200:1. O'Leary & Baughn (1977) estimated this ratio to be 5000:1.

References

Bossa, F., Martini, F., Barra, D., Borri Voltattorni, C., Minelli, A. & Turano, C. (1977) *Biochem. Biophys. Res. Commun.* **78**, 177–184

Borri Voltattorni, C., Minelli, A. & Turano, C. (1971) *FEBS Lett.* **17**, 231–235

Borri Voltattorni, C., Minelli, A., Vecchini, P., Fiori, A. & Turano, C. (1979) *Eur. J. Biochem.* in the press

Braunstein, A. E. (1973) *Enzymes 3rd Ed.* **9**, 379–480

Christenson, J., Dairman, W. & Uden Friend, S. (1972) *Proc. Natl. Acad. Sci. U.S.A.* **69**, 343–347

Fasella, P. (1967) *Annu. Rev. Biochem.* **36**, 185–210

Feldmann, K. & Helmreich, E. J. M. (1976) *Biochemistry* **15**, 2394–2401

Fiori, A., Turano, C., Borri Voltattorni, C., Minelli, A. & Codini, M. (1975) *FEBS Lett.* **54**, 122–124

Fisher, T. L. & Metzler, D. E. (1969) *J. Am. Chem. Soc.* **91**, 5323–5328

Gani, V., Kupfer, A. & Shaltiel, S. (1978) *Biochemistry* **17**, 1294–1300

Heinert, D. & Martell, A. E. (1963) *J. Am. Chem. Soc.* **85**, 183–188

John, R. A., Charteris, A. & Fowler, L. J. (1978) *Biochem. J.* **171**, 771–779

Johnson, R. J. & Metzler, D. E. (1970) *Methods Enzymol.* **18a**, 433–471

Lancaster, G. A. & Sourkes, T. L. (1972) *Can. J. Biochem.* **50**, 791–797

Matsushima, Y. & Martell, A. E. (1967a) *J. Am. Chem. Soc.* **89**, 1331–1335

Matsushima, Y. & Martell, A. E. (1967b) *J. Am. Chem. Soc.* **89**, 1322–1330

O'Leary, M. H. (1971) *Biochem. Biophys. Acta* **242**, 484–492

O'Leary, M. H. & Baughn, R. L. (1975) *Nature (London)* **253**, 52–53

O'Leary, M. H. & Baughn, R. L. (1977) *J. Biol. Chem.* **252**, 7168–7173

Peterson, A. B. & Sober, H. A. (1954) *J. Am. Chem. Soc.* **76**, 169–175

Pictet, A. & Spengler, T. (1911) *Ber.* **44**, 2030–2036

Schirch, L. & Jenkins, W. T. (1964) *J. Biol. Chem.* **239**, 3801–3807

Schott, H. E. & Clark, W. G. (1952) *J. Biol. Chem.* **196**, 449–462

Shukuya, R. & Schwert, G. W. (1960) *J. Biol. Chem.* **235**, 1653–1657

Stecher, P. G. (1968) *The Merck Index*, 8th edn., p. 397, Merck and Co., Rahway, NJ

Whaley, W. M. & Govindachari, T. R. (1951) *Org. React.* **6**, 151–190

Wilkinson, G. N. (1961) *Biochem J.* **80**, 324–332